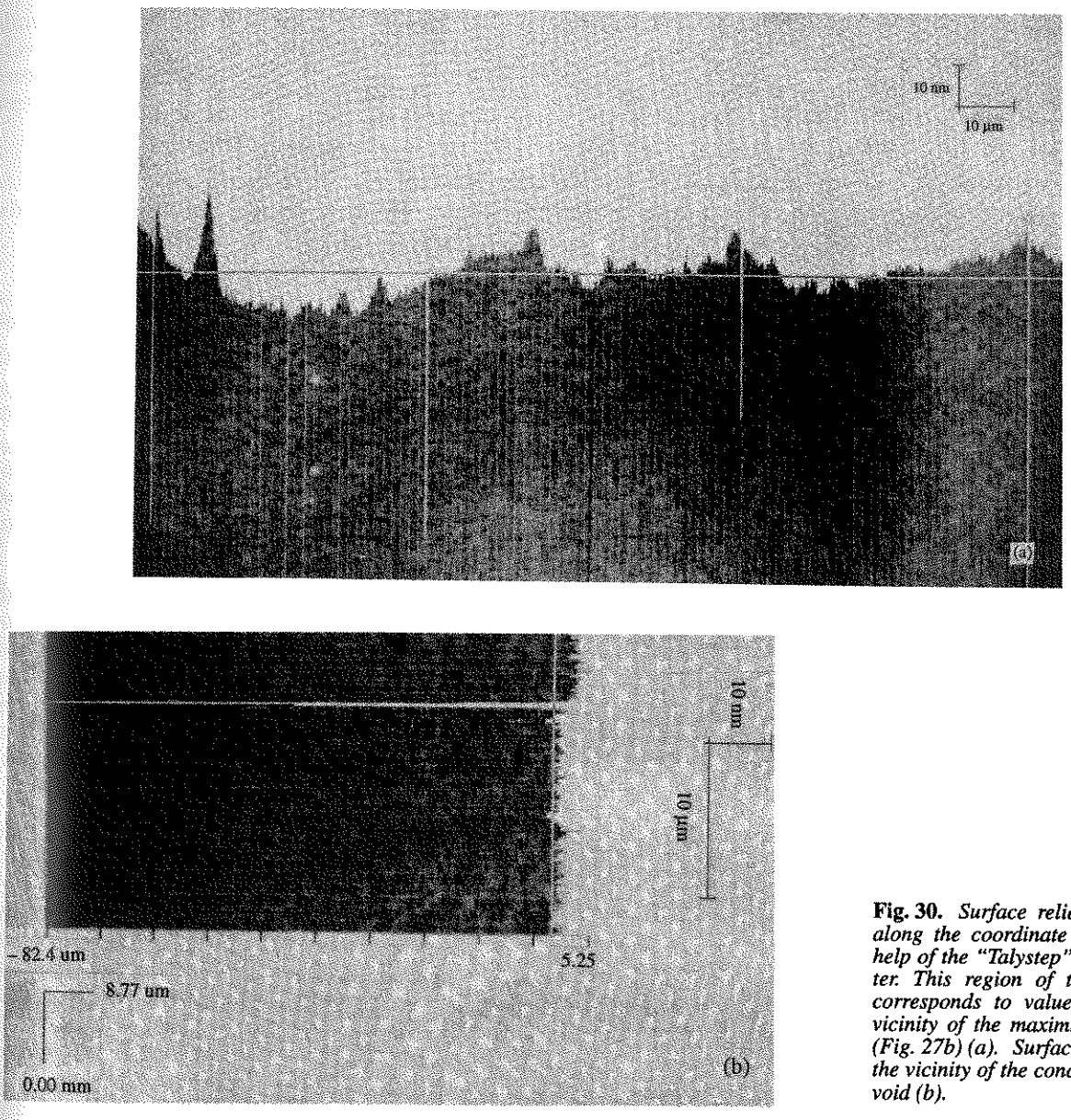

Fig. 30. *Surface relief recorded along the coordinate r with the help of the "Talystep" profilometer. This region of the surface corresponds to values r in the vicinity of the maximum of N(r) (Fig. 27b) (a). Surface relief in the vicinity of the concentric ring void (b).*

halves of the film. This gives rise to vacancy fluxes which are directed from the expanded regions into compressed ones. From Eqs. (6.3) and (6.4) it follows that the void flux is linked to the vacancy flux and is oppositely directed. As is seen from Fig. 26b, the voids pileup at the interface at the points of maximum dilation, decreasing there the local value of $\sigma_\perp$. From Fig. 26b one sees that this leads to a modulation of $\sigma_\perp$ along the film, which enhances the initial bending fluctuation, thus creating the positive feedback. The damage and de-adherence of the film from the substrate occurs along such void piles.

In the upper half of the film, as is seen from Eqs. (6.9) and (6.11), where $g < 0$, the feedback is negative and the void DDI does not develop. In accordance with Eq. (6.9) the de-adherence of the film must proceed in the form of the concentric rings, which is in fact observed in the experiment (cf. Fig. 31). In the upper half of the periodically bent film, the vacancy fluxes are directed into compressed regions, leading to a formation of the periodic ring void channels which are spatially synchronized with the positions of void piles in the lower half of the film (Fig. 26). It is these very narrow void channels that are recorded by a profilometer (Fig. 30).

The channel regions are optically transparent, which explains the luminous rings observed in the light transmission experiments (Fig. 31).

We shall now demonstrate the quantitative accordance of the DDI void theory with experimental results. Taking $\sigma_\perp = \sigma_\parallel \approx 10^8$ dyn·cm^{-2}, $N_0 S_0 = 3 \times 10^{-3}$ [19], $|\theta| = 10^{-11}$ erg, $T = 5 \times 10^2$ K we have in Eq. (6.15) $b / D \geq 1$. Thus the threshold condition (6.15) for DDI can be fulfilled under real conditions.

Let us demonstrate now the adequacy of the formulae for the period (6.14) and the growth rate (6.12) in the actual experiment. For the values mentioned

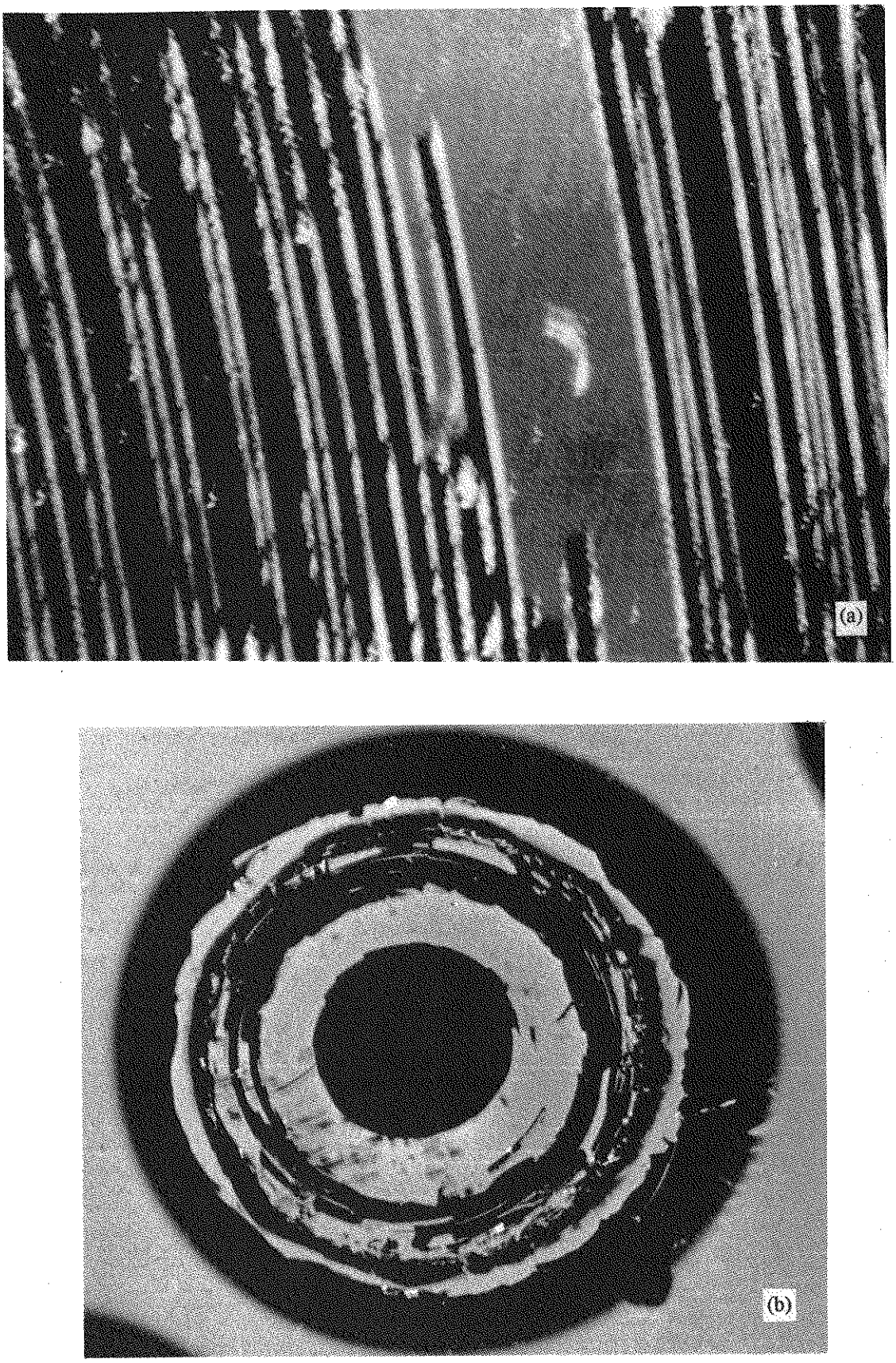

Fig. 31. *Concentric ring de-adherence of the film in the vicinity of the maximum value of N(r): the beginning of de-adherence (a); the detached film (b).*

above and $h \approx 5 \times 10^{-6}$ cm we have in Eq. (6.14) $l_0^2 = 5 \times 10^{-8}$ cm^2; for d in Eq. (6.14) we use the experimental value $d = d_{exp} = 3 \times 10^{-3}$ cm. From Eq. (6.14) we then obtain

$$b / D = (1 + \delta)^2,$$

where

$$\delta = 4\pi^2 l_0^2 / d^2 \cong 0.2.$$

For the growth rate (6.12) we then have $\lambda_{max} = D\delta^2 l_0^{-2}$. Putting in this formula $D = D_v n_{v0} a^3 \cong 10^{-8}$ cm^2·s^{-1} ($n_{v0}a^3 \sim 10^{-2}$, $D_v \sim 10^{-6}$ cm^2·s^{-1} [128]), one has $\lambda_{max}^{-1} \cong 10^2$ s, which is approximately equal to the experimental deposition time, after which the quasiperiodic de-adherence of the film begins. Thus, the deposition duration t_0 turned out to be long enough for the DDI void development.

An important conclusion which follows from the above theory is that the void DDI (and consequently the void ring formation) can be developed only when the film thickness satisfies the condition $h_{1cr} < h < h_{2cr}$ (see Eq. (6.17) and Fig. 27). This qualitative conclusion corresponds to the experiment (compare Fig. 27 and Fig. 32) and this fact strongly supports the DDI void theory.

In conclusion of this section we note that from the practical point of view, the effect of the concentric macrovoid formation discovered in Ref. [127] represents a unique method of obtaining very narrow microchannels with widths $\Delta r < 0.1$ μm in thin metallic films. On the other hand, the occurrence of the above-discussed instability hinders further growth of the film, because of the onset of film de-adherence from the substrate. To avoid this effect one can use a vapor deposition regime that minimizes the number of macrovoids N_0, such that the threshold condition (6.15) is not fulfilled. One possibility consists in a slow deposition (at least at the initial stage) which ensures that the number of through voids is minimal [19].

7. DISLOCATION-DIFFUSION-DEFORMATIONAL INSTABILITY

Similar to the field of point defects, the dense dislocation field, generated by external energy beams (in particular, laser ones) can become unstable with respect to transition to a spatially ordered state, coupled with periodic deformational state of the elastic continuum. The dislocation-deformational instability (DiDI) can develop due to two different mechanisms. The dislocation glide occurs in a self-consistent shear deformation field and leads to the formation of in-plane dislocation structure (Sec. 7.1). Dislocation climb occurs in the self-consistent strain field and leads to the formation of qualitatively different interplane dislocation structure (Sec. 7.2).

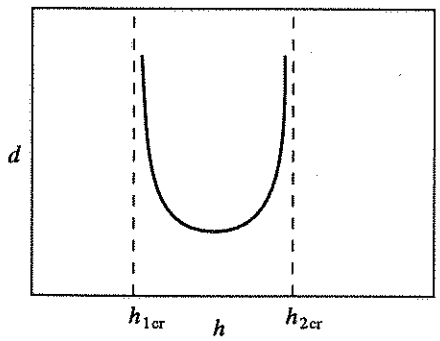

Fig. 32. *Period d of the dominant structure as a function of film thickness h for temperature T = const. The values h_{1cr} and h_{2cr} correspond to periods $d \to \infty$.*

7.1. Formation of In-Plane Periodic Dislocation-Shear Deformation Structures Due to Glide

7.1.1. Gliding Plane Lying in the Bulk of a Solid [29]

We consider first the DiDI due to the glide in the bulk of a solid. Let some plane (x, y) in the bulk of the medium be the gliding plane of the edge dislocations, elongated in the y direction with the Burgess vectors **b** directed along the x-axis. We introduce the number density of dislocation lines

$$\rho(x, z) = \sum_i \delta(x - x_i)\,\delta(z - z_i),$$

where the summation is carried out over all dislocations with $\mathbf{b} \parallel x$.

The dislocations move along the x-axis due to diffusion [129] and deformation-induced drift, so that the equation for ρ has the form

$$\frac{\partial \rho}{\partial t} = D_d \frac{\partial^2 \rho}{\partial x^2} - \frac{\partial}{\partial x}(\rho v). \tag{7.1}$$

Here D_d is the dislocation diffusion coefficient, v is the drift velocity

$$v = v_x = M\varepsilon^m, \tag{7.2}$$

where M and N are the constants ($m > 0$), ε is the shear deformation. This system of equations is completed by the equation for the displacement vector of the medium, which we treat for simplicity in isotropic approximation. In the considered geometry we have $U_x = 0$ and $\partial^2 U_z / \partial z^2 = 0$, so that

$$\partial^2 U_z/\partial t^2 = c_t^2 (\partial^2 U_z/\partial x^2) + c_t^2 \beta_a \frac{\partial^2 U_z^3}{\partial x^2} + \mathbf{b} c_t^2 \rho, \tag{7.3}$$

where β_a is the constant of elastic anharmonicity.

In the linear stability analysis we represent the variables in the form

$$\rho = \rho_0 + \rho_1, \quad v = v_0 + v_1, \quad \varepsilon = \varepsilon_0 + \varepsilon_1,$$

where ρ_0, v_0, and ε_0 are the spatially uniform variables and ρ_1, v_1, and ε_1 are the nonuniform perturbations. We assume that the variables ρ_0 and ε_0 are determined by the external pump intensity and hence are the control parameters of the DiDI.

Then, linearizing Eqs. (7.1 - 7.3) and neglecting the term with β_a in Eq. (7.3), we obtain the system of equations

$$\partial^2 U_{1z}/\partial t^2 = c_t^2 (\partial^2 U_{1z}/\partial x^2) + \mathbf{b}\rho_1, \quad (7.4)$$

$$\partial \rho_1/\partial t = D_d (\partial^2 \rho_1/\partial x^2) - g (\partial^2 U_{1z}/\partial x^2), \quad (7.5)$$

where the constant of coupling of the elastic continuum with the dislocation density field

$$g = m\rho_0 v_0 \varepsilon_0^{-1} \quad (7.6)$$

serves as the combined control parameter, depending on the pump intensity.

We develop the solution to the system (7.4) and (7.5) in the form

$$U_{1z} = A_q \exp(iqx + \lambda t), \ \rho_1 = B_q \exp(iqx + \lambda t), \quad (7.7)$$

where A and B are the initial amplitudes. The solution of the corresponding dispersion equation under the condition $q^2 c_t^2 \gg \lambda^2$ has the form

$$\lambda = g\mathbf{b} - D_d q^2 = m\rho_0 v_0 \varepsilon_0^{-1}\mathbf{b} - D_d q^2. \quad (7.8)$$

At $g\mathbf{b} \geq D_d q^2$ the growth rate $\lambda \geq 0$ and the DiDI develops with the fluctuations U_{1z} and ρ_1 growing in time. The stabilization of DiDI occurs due to the anharmonicity of the elastic continuum. In the stationary case from Eqs. (7.1) and (7.3), where $\lambda = 0$, one finds the equation for the stationary amplitude

$$-q^2 A_q - \beta_a q^2 |A_q|^2 A_q + \mathbf{b} g D_d^{-1} A_q = 0, \quad (7.9)$$

the solution of which at $\mathbf{b}g \geq D_d q^2$ has the form

$$|A_q| = \beta_a^{-1/2} ((\mathbf{b}g/D_d q^2) - 1)^{1/2}, \quad (7.10)$$

where $q \leq q_0 = (\mathbf{b}q / D_d)^{1/2}$.

The resultant DiD structure is determined by the sum over the wave numbers of all Fourier harmonics. With account for Eq. (7.7) we obtain for the resultant component of displacement vector

$$U_{1z} = \sum_{q \leq q_0} A_q \exp(iqx) \quad (7.11)$$
$$\approx \int_0^{q_0} q ((\mathbf{b}g/D_d q^2) - 1)^{1/2} \cos(qx)\, dq \backsim J_1(q_0 x).$$

The resultant shear deformation is $\partial U_z / \partial x \sim J_0(q_0 x)$. The dislocation density due to Eq. (7.5), where $\partial \rho_1 / \partial t = 0$ is

$$\rho_1(x) = \frac{g}{D_d} U_{1z}(x). \quad (7.12)$$

Thus, as a result of DiDI, coupled and spatially synchronized quasilocal periodic structures of shear deformation and dislocation density are formed in the gliding plane in the bulk of the medium. The period of these structures is

$$d = 2\pi/q_0 = 2\pi (D_d/\mathbf{b}g)^{1/2}. \quad (7.13)$$

In this derivation we have used the approximation of the isotropic elastic continuum. The anisotropy of the crystal in this simple model of DiDI is taken into account while selecting the axis of easiest gliding (x-axis).

7.1.2. Gliding Plane Lying on the Surface of a Solid [102]

Now let the gliding plane (x, y) with $z = 0$ be the surface plane of the material (z-axis is directed inside the medium). We consider the simplest one-dimensional model of self-organization of the edge dislocations with the dislocation lines lying in the gliding plane (similar to Sec. 7.1.1), occurring due to the interdislocation interaction through the elastic fields. We assume that due to laser beam action the dislocation field is generated in the subsurface layer, the density of which is described by the function

$$\rho(x, z) = \sum_i \delta(x - x_i)\, \delta(z - z_i)\, e^{-\gamma_d z}. \quad (7.14)$$

We shall describe the dislocation field by the same Eq. (7.1) as above. The feedback link of the DiDI is locked through the surface deformation due to the nonuniform dislocation distribution, given by Eq. (7.14) [100]

$$\varepsilon(x)|_{z=0} = (\mathbf{b}/4\pi(1-\sigma)) \int_0^{+\infty} dz \int_{-\infty}^{+\infty} dx' \rho(x', z) \quad (7.15)$$
$$\times (\xi(\xi^2 - z^2)/(\xi^2 + z^2)^2), \ \xi = x' - x,$$

where σ is the Poisson coefficient.

Eqs. (7.1), (7.2), and (7.15) are the closed system of equations under the assumption that $\gamma_d \gg d^{-1}$, where d is the period of the DiD structure. Under this condition the variable $v = v_x$ in Eq. (7.1) is the drift velocity on the surface $v_x|_{z=0}$.

We represent the variables in a form similar to Eq. (7.7) and substitute them into the linearized Eqs. (7.1) and (7.15). With $\rho_1 \sim e^{iqx - \gamma_d z}$ an integral in the right-hand side of Eq. (7.15) can be easily calculated, and as a result one obtains the growth rate ($\gamma \gg q$):

$$\lambda = -D_d q^2 + q \frac{g\mathbf{b}}{2\gamma_d (1-\sigma)}. \quad (7.16)$$

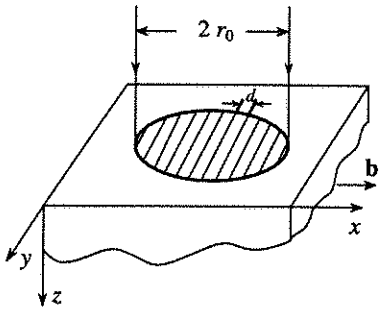

Fig. 33. *Geometry of the formation of periodic dislocation structures. b is a Burgess vector of wedge dislocation elongated in the y-direction (a); the profile of the deformed surface (b).*

It is seen that the dependence $\lambda = \lambda(q)$ in the case of the surface DiDI has a maximum opposite to the case of the bulk one (cf. Eqs. (7.16) and (7.8)). Thus one may expect the formation of a well-developed long-order surface DiD structures.

The maximum is reached at

$$q = q_{\max} = \frac{g\mathbf{b}}{4D_d\gamma_d(1-\sigma)},$$

so that the period of the surface DiDI is

$$d = \frac{2\pi}{q_{\max}} = \frac{8\pi(1-\sigma)D_d\gamma_d}{\mathbf{b}g}. \qquad (7.17)$$

The characteristic time of the DiDI grating formation ($t_d \simeq \lambda_{\max}^{-1}$) is

$$t_d \simeq \frac{d^2}{4\pi^2 D_d}. \qquad (7.18)$$

As in the case of bulk DiDI the x-axis is the axis of easiest glide. There are two such axes on the surface (100), so that two mutually perpendicular DiD gratings must be formed.

Let us see whether the mechanism of dislocation DDI can explain the experimental results of Sec. 4.3.1 on formation of surface grating with a period $d \sim 3$ μm under millisecond laser excitation ($t_d \lesssim 10^{-3}$ s). From the scaling relation (7.18) we have for the necessary value of dislocation diffusion coefficient $D_d \gtrsim 10^{-6}$ cm^2·s^{-1}. These values of the diffusion coefficient are characteristic for point defects (vacancies) and far too large for extended defects. Hence the dislocation DDI is too slow of a process to be responsible for millisecond grating formation. Thus, we conclude that the point defect DDI, considered in Sec. 4.3.2, is the only possible mechanism left for explaining the experimental results of Sec. 4.3.2.

The characteristic feature of surface dislocation gratings formed due to in-plane DiDI is that the lines of dislocation pileups are not quite straight due to the finite length of dislocation comprising them (the so-called "vein" structures [13]; for illustration see Fig. 34, contrary to the ideally straight lines in the case of the interplane DiD structure (see Fig. 35).

We have described above the formation of "vein" structures in the framework of the dislocation DDI model. Note that previously such structures were described in the model of the diffusion-reaction equation, assuming that there are two types of dislocations: mobile and immobile ones interacting with each other [131, 132]. The consideration of this section shows that dislocation ordering can occur in the system of mobile dislocations due to DDI.

7.2. Formation of Interplane Periodic Dislocation-Strain Structure Due to Climb

In interplane DiDI the dislocation ordering occurs due to the dislocation redistribution between the different atomic planes as a result of deformation-induced drift of vacancies (or interstitials). The intersections of atomic planes saturated with dislocation lines with the surface plane yields the structure of periodic and ideally straight lines on the surface, which in fact are the valleys of surface relief, corrugated due to DiDI (see below).

The formation of such a structure was recorded, for example, in Ref. [134]. A plate of crystalline Si, 50-mm diameter and $H = 1$ mm thickness with (111) orientation was installed in a vacuum chamber (10^{-3} torr). The cw radiation from a Nd : YAG laser ($\lambda = 1.06$ μm, $P = 100$ W) was focused into a spot of radius $r_0 = 5 \times 10^{-2}$ cm and heated the surface for 60 s.

Microscope investigation of the surface opposite the irradiated one revealed the presence in the region $r \lesssim 5 \times 10^{-1}$ cm of a whole set of periodic structures, composed of straight lines, oriented at angles 60° to each other. The distance between the lines was $d \simeq 10^{-4}$ cm (Fig. 35a). When the carbonil ($Mo(CO)_6$) vapors were let in to the camera the deposition of the thin Mo film took place. The relief of the film surface corresponded to the picture of the surface periodic line structure (Fig. 35b). Note that similar dislocation gratings were observed also on the surface treated by the scanning CO_2-laser radiation in Ref. [135].

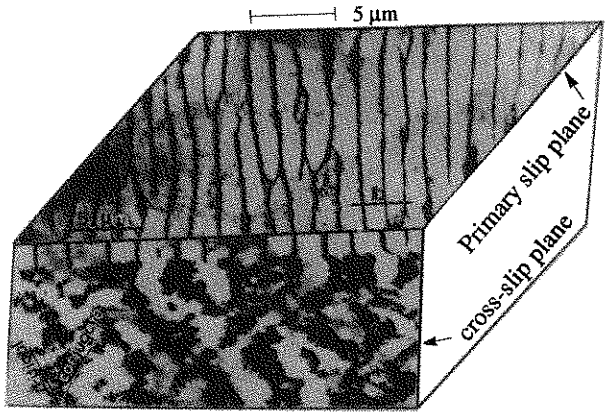

Fig. 34. *The periodic "vien" dislocation structure formed under multipulse mechanical deformation of the surface [133].*

Let us consider the model of DiDI due to dislocation climb, which explains this phenomenon. We assume that due to some generation process (thermal deformation or point defect condensation) the edge dislocations arise in the subsurface layers with the orientations shown in Fig. 36. The gliding of these dislocations in the (100) planes leads to formation of traces on the (111) plane in the form of three sets of straight lines crossing at angles 60° with respect to each other. We consider one of these sets and denote the axis perpendicular to the lines of this set by $0x$ (Figs. 36 and 37).

The appearance of density of dislocations spatially nonuniform along x leads to the appearance of coupled spatially synchronized distribution of strain div $\mathbf{U}(x)$. In its turn, the latter leads to the appearance of deformation-induced vacancy fluxes, the sources and the sinks of which are the dislocation lines

$$\mathbf{j}_v = -D_v \frac{\partial}{\partial x} n_v + n_v D_v \frac{|\theta_v|}{kT} \frac{\partial}{\partial x} \operatorname{div} \mathbf{U}. \qquad (7.19)$$

Due to the vacancy fluxes there appears the dislocation flux. Contrary to the case of voids (see Sec. 6.1) the dislocation flux has the same direction as vacancy flux

$$\mathbf{j}_d = \rho_d \mathbf{V}_d = \rho_d a^3 \mathbf{j}_v. \qquad (7.20)$$

Using the continuity equation for dislocation density and the adiabatic relation $\rho_d = \text{const}\ n_v$ (compare with Sec. 6.1) we obtain the equation for number density of dislocations

$$\frac{\partial \rho_d}{\partial t} = D \frac{\partial^2 \rho_d}{\partial x^2} - \frac{\rho_d |\theta_v| D}{kT} \frac{\partial^2}{\partial x^2} (\operatorname{div} \mathbf{U}_f)\big|_{z=0} + G_d, \qquad (7.21)$$

where $D = D_v n_v a^3$ is the effective diffusion coefficient of dislocations, G_d is the dislocation generation rate uniform along x, $\mathbf{U}_f$ is the displacement vector of the medium saturated with dislocations.

This dislocation saturated subsurface layer with a thickness of the order of the length of dislocation (dislocation semiloop) h has the density ρ_f different from that of the bulk. We consider this surface layer as a film with a thickness h on the substrate (the z-axis is directed into the substrate, the $z = 0$ plane being the film-substrate interface plane) (Fig. 37). Thus, once again we use the film-on-substrate model used previously in Sec. 4.3.2. The basic equations are similar to those used in Sec. 4.3.2. They are the equations for the bending coordinate of the film ζ:

$$\frac{\partial^2 \zeta}{\partial t^2} + c^2 l_0^2 \frac{\partial^4 \zeta}{\partial x^4} = \frac{\sigma_\perp}{\rho_f h}. \qquad (7.22)$$

The equation for the subsurface layer strain

$$\operatorname{div} \mathbf{U}_f = -\nu (z + h/2) \frac{\partial^2 \zeta}{\partial x^2}, \qquad (7.23)$$

the equation for the displacement vector of the substrate

$$\frac{\partial^2 \mathbf{U}}{\partial t^2} = c_t^2 \Delta \mathbf{U} + (c_l^2 - c_t^2) \operatorname{graddiv} \mathbf{U} \qquad (7.24)$$

with the boundary conditions at interface

$$U_z|_{z=0} = \zeta, \qquad (7.25)$$

$$\mu \left(\frac{\partial U_x}{\partial z} + \frac{\partial U_z}{\partial x} \right)\Big|_{z=0} = h \theta_{dis} \frac{\partial \rho_d}{\partial x}, \qquad (7.26)$$

$$\theta_{dis} = Kah,$$

$$\left(\frac{\partial U_z}{\partial z} + (1 - 2\beta) \frac{\partial U_x}{\partial x} \right)\Big|_{z=0} = \frac{\sigma_\perp}{\rho c_l^2}. \qquad (7.27)$$

In writing Eq. (7.26) we used the relation $\sigma_{xz} = \partial f / \partial x$ [136], where $f = h\theta_d \rho_d$. The system of Eqs. (7.21 - 7.27) is completely analogous to the system (4.57 - 4.63), so that we can immediately use the results, obtained in Sec. 4.3.2, adapting them to the case considered here.

The solution of Eqs. (7.21 - 7.27) has the form

$$\rho_d = \rho_{d0} + \rho_{d1} e^{iqx + \lambda t}, \quad \zeta = \zeta_1 e^{iqx + \lambda t},$$

where ρ_{d0} is the spatially uniform part, and the displacement vector in the substrate is given by Eq. (4.65c).

The growth rate

$$\lambda = -Dq^2 + q^4 \frac{g}{1 + \alpha h^3 q^3}, \qquad (7.28)$$

where

$$\alpha = \frac{1}{24} \frac{\rho_f}{\rho} \frac{c^2}{c_t^2} \frac{1}{1 - \beta}, \quad g = \rho_{d_0} \frac{|\theta_v \theta_{dis}| \beta h^2 \nu D}{4 (1 - \beta) \mu kT} \equiv \rho_{d_0} A;$$

$$\beta = c_t^2 / c_l^2.$$

At $\lambda > 0$ the DiDI is accompanied by the formation of the dislocation density grating, periodic bending of the subsurface layer and deformation of the elastic continuum of the substrate. The period of DiD grating is $d = 2\pi / q_{max}$, where q_{max} is the value of q at which the maximum of $\lambda(q)$ is reached. Under the condition $\alpha h^3 q^3 \gg 1$ from Eq. (7.28) we obtain

$$d \equiv \frac{2\pi}{3} \left(\frac{\mu}{K} \right) \left(\frac{\rho_f}{\rho} \right) \left(\frac{c^2}{c_t^2} \right) \left(\frac{kT}{Ka^3} \right) \left(\frac{1}{\rho_{d_0} a} \right) \sim \left(\frac{kT}{Ka^3} \right) \frac{1}{\rho_{d_0} a}. \qquad (7.29)$$

The DiDI occurs when the mean density of dislocations exceeds the critical value

$$\rho_d > \rho_{dcr} \equiv (\alpha h^3 / A)\, Dq.$$

At $K = 10^{12}$ erg·cm^{-3}, $a = 5 \times 10^{-8}$ cm, $\mu \approx K$, $\rho_f \approx \rho$, $\beta = 1$, $c^2 \approx c_t^2$, $T = 10^3$ K, $\rho_{dcr} = 10^8$ cm^{-2} from Eq. (7.29) we obtain the value of the period $d \sim 10^{-4}$ cm, which corresponds to the experimental value. At $d \sim 10^{-4}$ cm the critical density of dislocations at which the DiDI due to climb occurs is $\rho_{dcr} \sim 5 \times 10^7$ cm^{-2}.

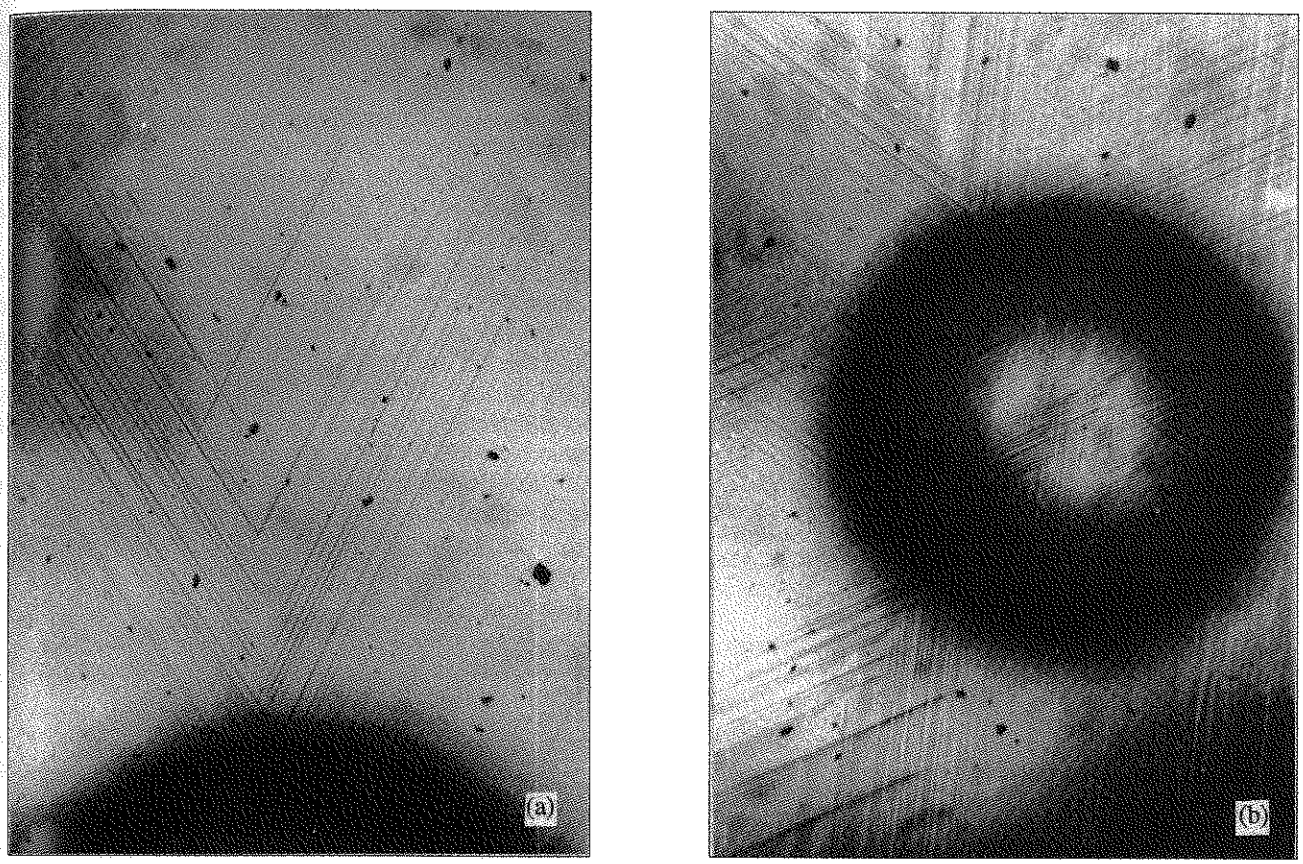

Fig. 35. *Periodic dislocation structures on (111) surface of Si (a). The deposited metal film follows the ordered dislocation structure (b).*

Let us discuss the physical mechanism of DiDI. Let the fluctuation Fourier harmonic of dislocation density arise in the film. Due to Eq. (7.26) this leads to appearance of the shear deformation in the substrate, and due to Eq. (7.27), the appearance of stress $\sigma_{\perp}$, perpendicular to the interface. Owing to Eq. (7.22), this gives rise to the harmonic of bending deformation and occurrence of harmonic of strain (7.23) in the film. The arising deformation-induced flux of vacancies leads to the dislocation climb along the x direction, which is accounted for in Eq. (7.21).

This climb leads to spatial redistribution of dislocations along the x direction, which enhances initial fluctuation of dislocation density spatial harmonic and at $\rho_d > \rho_{dcr}$ leads to the onset of DiDI. We see that the DiDI due to dislocation climb is similar to void-deformational instability in films, considered in Sec. 6.1.

8. EXOTHERMAL CRYSTALLIZATION-DEFORMATION-THERMAL INSTABILITY AND FORMATION OF ORDERED PHASE STRUCTURES

All instabilities considered in this review up to now are the endothermal processes developing due to the energy absorbed from an external source. This is seen from the fact that the growth rate of these instabilities is proportional either to some power of intensity of the exciting laser beam, as in the case of EDTI (Sec. 2), or to the number density of point defects n_{d0} (Secs. 4 and 5) or extended defects (Secs. 6 and 7), generated by an external pump. In this section we consider the example of exothermal crystallization-deformation-thermal instability (CDTI), occurring in amorphous materials (semiconductors) due to the latent heat of crystallization. Laser radiation serves only as an initial activator of the EDTI. In Sec. 8.1 we study the CDTI on the surface of the amorphous material, irradiated by a laser beam, and in Sec. 8.2 we consider the case of CDTI in a film.

8.1. Surfaces of Amorphous Solids

The processes of crystallization of surface layers of amorphous semiconductors under the action of pulsed laser radiation (with pulse duration $\tau_p = 10^{-11} - 10^{-8}$ s) are being currently widely investigated [139 - 141]. After laser irradiation the periodic structures formed by the alternation of crystalline and amorphous concentric ring structures are often recorded on the surfaces, with the number of the rings being as many as five [38] to eight [143]. For irradiation of amorphous Ge films, formation of more sophisticated periodic structures with concentric rings and radial rays ("star"-like structures) was observed (see Refs. [140, 144] and Fig. 38). The

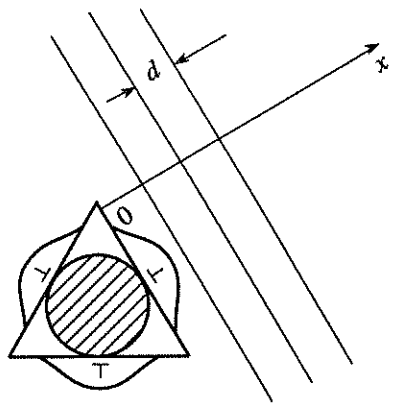

Fig. 36. *Ordered laser-induced interplane dislocation structure on the (111) surface. The dashed region is the laser spot. The thermal deformation of atomic planes and configuration of dislocations arising are shown. d is the dislocation grating period.*

formation of these periodic structures evidences the development of a certain instability on the irradiated surface. In some cases this may be endothermal surface EDTI due to the interband transitions in semiconductors, described in Secs. 2 and 3.4.

In this section we consider another type of laser-induced instability on the surfaces of amorphous materials, leading to formation of the periodic phase structures – exothermal CDTI [144].

The physical mechanism of CDTI on the surface consists in the following. An amorphous phase is a metastable state with stored internal energy – the hidden crystallization energy. The rate of crystallization at room temperatures and in the absence of deformations is infinitesimally small. With laser heating up to temperature $T \lesssim T_m$ (T_m being the melting temperature) this rate is locally enhanced. The fluctuation harmonic of deformation of the surface layer spatially modulates the crystallization rate. This is accompanied by the spatial modulation of the hidden heat extraction and due to this by the spatial modulation of temperature.

Due to the inhomogeneous (along the surface) temperature field T arising, there appears the thermal elastic force $\mathbf{F} \sim \text{grad } T$, which enhances the initial deformation. The positive feedback arising under certain conditions leads at $T > T_{cr}$ (T_{cr} is a critical temperature) to the instability in which the Fourier amplitudes of the temperature-induced static surface deformation and also of crystallization rate grow exponentially in time.

One of the conditions of CDTI is the absence of melting. We stress the fact that the laser heating (pulsed or cw) in the CDTI plays the role of initial activation and the instability itself develops due to the hidden crystallization heat. This is the principal difference between the CDTI and the endothermal EDTI on the surfaces of semiconductors (Sec. 2), which also leads to formation of similar periodic deformation structures, but develops due to absorbed laser pulse energy. The leading role of deformations distinguishes CDTI from the usual explosive crystallization, occurring due to thermal effects only [139, 140].

As a result of development of the CDTI the concentric ring-shaped temperature and deformation fields and the resultant ring or star structures of periodically alternate amorphous and crystalline phases are formed (Figs. 2 and 38).

Apart from the complicated periodic structures, formation of simpler structures consisting of a crystalline spot in the center and one crystalline ring with a radius of the order of the dimension of the laser spot were recorded under picosecond irradiation of amorphous semiconductors [142, 145, 146]. The dynamics of their formation shows that it occurs due to Gaussian distribution of intensity in the laser beam cross-section and not due to development of instability.

The CDTI considered in the present section can arise not only under laser irradiation but also under electron beam irradiation or even under heating by a furnace. It is interesting to note that in the latter case a concentric ring and more sophisticated radial-ring periodic phase structures are created [147].

We consider an amorphous medium filling a semispace $z \geq 0$. Let $a = a(x, y)$ denotes the local relative volume of amorphous phase with

$$a = \Delta v_a / \Delta v,$$

where Δv is a physically small volume, Δv_a and Δv_c are the volumes of amorphous and crystalline phases, respectively. The variable a obeys the activation kinetic equation

$$\frac{da}{dt} = -\frac{a}{\tau_0} \exp\left(-\frac{W + \theta \operatorname{div} \mathbf{U}}{kT}\right); \quad \theta < 0. \tag{8.1}$$

Here W is the activation energy, τ_0 is the phenomenological constant, θ is the deformational potential, $\mathbf{U}$ is the displacement vector. Eq. (8.1), where $\theta = 0$, is usually used for the description of thermal explosive crystallization [152]. With $\theta \neq 0$ Eq. (8.1) takes into account the fact that deformation modifies the crystallization rate.

The equation for T has the form (cf. Eq. (3.10))

$$\frac{\partial T}{\partial t} = \chi \Delta T + \frac{E_c}{\tau_0 c_v} a \exp\left(-\frac{W + \theta \operatorname{div} \mathbf{U}}{kT}\right) + \frac{c\gamma |E|^2 (1 - R)}{2\pi c_v} \exp(-\gamma z). \tag{8.2}$$

Here E_c is the hidden crystallization rate, E is the laser field amplitude.

The boundary conditions for Eq. (8.2) are given by formulas

$$\left(\frac{\partial T}{\partial z}\right)_{z=0} = 0, \quad (T - T_{init})_{\infty} = 0. \tag{8.3}$$

Eqs. (8.1) and (8.2) are closed by the equation for $\mathbf{U}$:

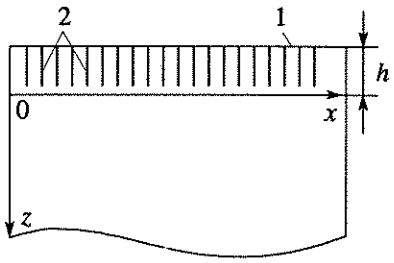

Fig. 37. *Model of the medium with the subsurface layer saturated with dislocations: the film of a thickness of the order of the dislocation length h on an elastic substrate. 1 – the Si plate surface, 2 – the dislocation semiloops.*

$$\frac{\partial^2 \mathbf{U}}{\partial t^2} = c_t^2 \Delta \mathbf{U} + (c_l^2 - c_t^2)\,\mathrm{grad\ div}\ \mathbf{U} - \frac{K\alpha}{\rho}\,\mathrm{grad}\ T, \tag{8.4}$$

ρ is the mean density of the medium (we neglect the difference between the densities of amorphous and crystalline phases). We put $\xi = \mathrm{div}\ \mathbf{U}$ and $T = T_0 + T_1$, $a = a_0 + a_1$, $\xi = \xi_0 + \xi_1$, where T_0, a_0, and ξ_0 are spatially uniform along the surface solutions and T_1, a_1, and ξ_1 are small spatially nonuniform perturbations.

Linearizing the expressions (8.1) and (8.2) with respect to perturbations, we obtain the equations of zero order

$$da_0/dt = -a_0\tau^{-1};\ \tau^{-1}(z) = \tau_0^{-1}\exp\left(-\frac{W_0}{kT_0}\right);\qquad W_0 = W + \theta\xi_0, \tag{8.5}$$

$$\frac{dT_0}{dt} = \chi\Delta T_0 + \frac{E_c}{\tau c_v}a_0 + \frac{c\gamma|E|^2}{2\pi c_v}\exp(-\gamma z) \tag{8.6}$$

and the equations of the first order

$$\frac{da_1}{dt} = -\frac{1}{\tau_0}\left[a_0\left(-\frac{\theta}{kT_0}\,\mathrm{div}\ \mathbf{U} + \frac{W_0}{kT_0^2}T_1\right) + a_1\right]\exp-\frac{W_0}{kT_0}, \tag{8.7}$$

$$\frac{\partial T_1}{\partial t} = \chi\Delta T_1 + \frac{E_c}{\tau_0 c_v}\left[a_0\left(\frac{W_0}{kT_0^2}T_1 - \frac{\theta}{kT_0}\,\mathrm{div}\ \mathbf{U}\right) + a_1\right]\exp\left(-\frac{W_0}{kT_0}\right). \tag{8.8}$$

We note that by neglecting the thermal conductivity ($\chi = 0$) one obtains from Eqs. (8.7) and (8.8) the law of energy conservation

$$\frac{\partial}{\partial t}(E_c a_1 + c_v T_1) = 0.$$

Expanding $\xi_0(t, z)$ in a power series

$$\xi_0(t) = \xi_0(0) - \xi_0' z,\quad \xi_0' = \left|\frac{\partial \xi_0}{\partial z}\right|$$

and using this expansion in Eqs. (8.7) and (8.8) one obtains

$$\exp\left[-\frac{W + \theta\xi_0(z)}{kT_0(z)}\right] \approx \exp\left[-\frac{W_0(0)}{kT_0(0)}\right]\exp\left[-\frac{|\theta|\,\xi_0'}{kT_0(0)}z\right]. \tag{8.9}$$

The approximation (8.9) is valid, if $|\theta| / kT(0) \gg \xi_0^{-1}$. Moreover, under the condition $\lambda\tau > 1$ one can neglect the term $\sim a_1$ in the right-hand side in Eqs. (8.7) and (8.8). Then, the Eq. (8.8) accounting for Eq. (8.9) acquires the form

$$\frac{\partial T_1}{\partial t} = \chi\Delta T_1 + g\,\mathrm{div}\ \mathbf{U}e^{-\Gamma z} + \sigma T_1 e^{-\Gamma z}, \tag{8.10}$$

where

$$g = \frac{1}{\tau(0)}\left(\frac{E_k}{c_v T_0(0)}\right)\left(\frac{W(0)}{kT_0(0)}\right)a_0 \equiv S\exp\left[-W_0(0)/(kT_0(0))\right]/(k^2T_0^2(0)); \tag{8.10a}$$

$$\Gamma = \left(\frac{|\theta|}{kT_0(0)}\right)\left|\frac{\partial\xi_0}{\partial z}\right|;\qquad \sigma = -\frac{T_0(0)}{\tau(0)}\left(\frac{E_k}{c_v T_0(0)}\right)\left(\frac{\theta}{kT_0(0)}\right)a_0. \tag{8.11}$$

Eqs. (8.10) and (8.4) constitute a closed system of equations for T_1 and $\mathbf{U}$, the solution of which determines the first order perturbation of the crystallization rate, in accordance with Eq. (8.7).

We assume that the change of T_1 and div $\mathbf{U}$ with the distance from the surface is small on the length Γ^{-1} (which is usually the case, see below). Then, in the last two terms on the right-hand side of Eq. (8.10) one can substitute $T_1(z) = T_1(0)$, $(\mathrm{div}\ \mathbf{U})_z = (\mathrm{div}\ \mathbf{U})_{z=0}$ and write

$$\frac{\partial T_1}{\partial t} - \chi\Delta T_1 = [g\,\mathrm{div}\ \mathbf{U} + \sigma T_1]_{z=0}\,e^{-\Gamma z}. \tag{8.12}$$

The system of Eqs. (8.4) and (8.12) describing CDTI is similar to Eqs. (2.4) and (2.8) of EDTI. The difference is that the coefficients $g \equiv \varepsilon_{T\xi}$ and $\sigma \equiv \varepsilon_{TT}$ are now proportional not to laser intensity as in Eq. (2.8), but to the latent crystallization heat E_c. The procedure for the solution of the system (8.4) and (8.12) is quite analogous to that carried out in Sec. 2.3. We consider explicitly the formation of concentric ring surface structures.

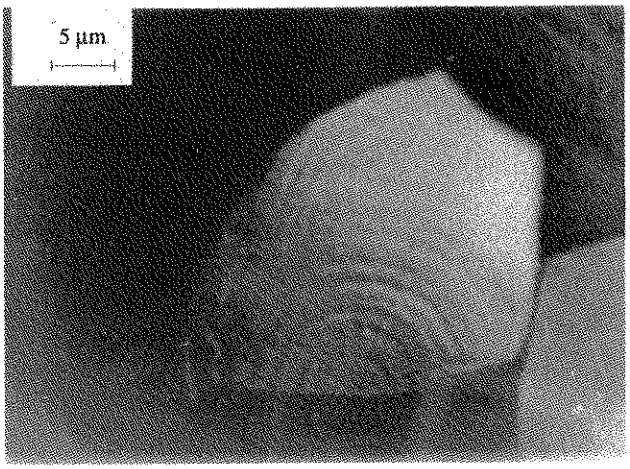

Fig. 38. *Surface structure of the "star" type, formed on the α–Ge film as a result of pulsed laser irradiation (photograph made with an optical microscope).*

The deformation on the surface in the form is given by

$$(\mathrm{div}\ \mathbf{U})_{z=0} = AJ_0(qr)\exp(\lambda t). \tag{8.13}$$

The solution of Eq. (8.12) with the boundary conditions (8.3) has the form

$$T_1 = \frac{\tilde{g}\exp(\lambda t)}{\chi(\Gamma^2-\delta^2)}AJ_0(qr) \times\left[\frac{\Gamma}{\delta}\exp(-\delta z)-\exp(-\Gamma z)\right], \tag{8.14}$$

where $\delta^2 = q^2+\lambda/\chi$, $\tilde{g} = g/(1-\sigma/(\chi\Gamma\delta))$. Under the condition $\delta \ll \Gamma$ one can neglect the second term in Eq. (8.14). Additionally, δ^{-1} determines the length of the T_1 decay with distance from the surface in accordance with the adopted approximation.

The explicit boundary conditions for $\mathbf{U}$ at the free surface have the form

$$\left(\frac{\partial U_r}{\partial z}+\frac{\partial U_z}{\partial r}\right)_{z=0} = 0, \tag{8.15}$$

$$\left[-\frac{K\alpha}{\rho c_1^2}T_1+\frac{\partial U_z}{\partial z}+(1-2\beta)\left(\frac{\partial U_r}{\partial r}+\frac{U_r}{r}\right)\right]_{z=0}=0, \qquad \beta = c_t^2/c_1^2. \tag{8.16}$$

Using the decomposition of $\mathbf{U} = \mathbf{U}_l + \mathbf{U}_t$ (Eq. (2.14)), we obtain the equations for $\mathbf{U}_l$ and $\mathbf{U}_t$

$$\frac{\partial^2\mathbf{U}_l}{\partial t^2} = c_l^2\Delta\mathbf{U}_l$$

$$-\frac{K\alpha A\tilde{g}}{\rho\chi\Gamma\delta}\,\mathrm{grad}\,(J_0(gr)\exp(-\delta z))\exp(\lambda t), \tag{8.17}$$

$$\frac{\partial^2\mathbf{U}_t}{\partial t^2} = c_t^2\Delta\mathbf{U}_t,$$

the solutions of which are developed in the form

$$U_{lr} = (b\exp(-\kappa_l z)+d\exp(-\delta z))J_{-1}(qr)\exp(\lambda t), \tag{8.18}$$

$$U_{lz} = (a\exp(-\kappa_l z)+f\exp(-\delta z))J_0(qr)\exp(\lambda t); \tag{8.19}$$

$$U_{tr} = -\kappa_t N J_{-1}(qr)\exp(-\kappa_t z+\lambda t), \tag{8.20}$$

$$U_{tz} = qNJ_0(qr)\exp(-\kappa_t z+\lambda t), \tag{8.21}$$

where a, b, f, d, and N are constants. Further calculations proceed similar to Sec. 2.3 (following Eq. (2.16)). Under the condition $\lambda^2/c_l^2 \ll (\delta^2-q^2)$ we find

$$A = \frac{\lambda^2}{c_l^2}M/[1-R/(\chi\Gamma\delta-\sigma)],$$

where M is some constant and

$$R = \frac{K\alpha E_c|\theta|a_0}{\rho c_l^2\tau_0 c_v kT_0(0)}\exp\left(-\frac{W_0(0)}{kT_0(0)}\right) \equiv Q\exp\left(-\frac{W_0(0)}{kT_0(0)}\right)/(kT_0(0)). \tag{8.22}$$

Taking into account Eqs. (8.18) and (8.21) one can express the solution of Eq. (19) in terms of the constants M and N

$$U_z = J_0(qr)\exp(\lambda t)\{M[-\kappa_l\exp(-\kappa_l z) + \frac{\lambda^2}{c_l^2}R\exp(-\delta z)/(\chi\Gamma(q^2-\delta^2) \times(1-(R+\delta)/\chi\Gamma\delta))]+Nq\exp[-\kappa_t z]\}, \tag{8.23}$$

$$U_r = J_{-1}(qr)\exp(\lambda t)\{M[q\exp(-\kappa_l z) - \frac{\lambda^2}{c_l^2}Rq\exp(-\delta z)/(\chi\Gamma(q^2-\delta^2) \times(1-(R+\sigma)/\chi\Gamma\delta))]-N\kappa_l\exp(-\kappa_t z)\}. \tag{8.24}$$

Now, from Eqs. (8.15), (8.16) and (8.23), (8.24), quite analogously to the derivation after Eq. (2.21) in Sec. 2.3, one obtains the dispersion equation for CDTI

$$(\kappa_t^2+q^2)^2-4\kappa_t\kappa_l q^2 = R\frac{\lambda^2}{c_1^2\chi\Gamma\delta}\frac{\left[(\kappa_t^2+q^2)^2-4\kappa_t\delta q^2\right]}{(q^2-\delta^2)\,[1-(R+\sigma)/(\chi\Gamma\delta)]}. \quad (8.25)$$

The structure of this equation is similar to that of the dispersion equation for EDTI (2.22). The parameter R in Eq. (8.25), given by Eq. (8.22), describes coupling between the deformational-thermal properties of the medium ($K\alpha$) and crystallization properties $(E_c/\tau_0)\exp(-W/kT_0(0))$ via the deformational potential θ.

First, we find the solution of the dispersion equation near the CDTI threshold, when $\lambda \to 0$. From Eq. (8.25) under the condition $\lambda/\chi q^2 \ll 1$ one obtains the soft CDT-mode

$$\lambda = -2\chi q^2 + 2\frac{q}{\Gamma}\left(\frac{R}{1-\beta}+\sigma\right). \quad (8.26)$$

In the region above the threshold, under the condition

$$\mu \equiv \frac{\lambda^2}{c_{l,t}^2 q^2},$$

expanding (8.25) into a power series of the parameter μ, we obtain the following simplified dispersion equation

$$(\delta+q)(\delta-q_{R\sigma}) = [2\beta/(1-\beta)]\,qq_R, \quad (8.27)$$

where $q_R \equiv R/(\chi\Gamma)$, $q_{R\sigma} \equiv (R+\sigma)/(\chi\Gamma)$, $(0 \le \beta \le 1/2)$. The solution of Eq. (8.27) has the form

$$\lambda = \chi\left[\left(\frac{(q+q_{R\sigma})^2}{4}+qq_R\frac{2\beta}{1-\beta}\right)^{1/2}+\frac{q_R-q}{2}\right]^2-\chi q^2. \quad (8.27a)$$

The dependence $\lambda = \lambda(q)$ according to Eqs. (8.27a) and (8.26) is shown in Fig. 39. When $R \gg \sigma$ the maximum value of the growth rate λ is reached at

$$q_{\max} = q_{R\sigma}\left[(5a^2+6a+1)^{1/2}-(2a+1)\right],$$
$$a \equiv \frac{2\beta}{1-\beta}\frac{q_R}{q_{R\sigma}},$$
$$\lambda_{\max} = \chi q_{R\sigma}^2\frac{1}{2}\left[(5a+1)(5a^2+6a+1)^{1/2}-11a^2-8a+1\right]. \quad (8.28)$$

The periodic ring structure with $q = q_{\max}$ and $\lambda = \lambda_{\max}$ is dominant in the overall situation of surface excitations.

At $\sigma \gg R$ ($q_{R\sigma} \gg q_R$) the growth rate is given by $\lambda = \chi(q_{R\sigma}^2 - q^2)$ and the maximum is achieved at $q = 0$ (Fig. 39). We want to show that the formation of periodic surface structures is possible also in this case.

To do so, let us find the dependence of the initial amplitude of surface deformation A in Eq. (8.13) on the wavenumber q. For one-dimensional grating $U_q \sim q^{-1}\cos qr$, whence $\operatorname{div}\mathbf{U}_q \sim \cos qr\cos\varphi$. Going over to the ring structure we have

$$\operatorname{div}\mathbf{U}_q \sim (1/\pi)\int_0^{\pi}\cos(qr\cos\varphi)\,d\varphi = J_0(qr),$$

i.e., in the Eq. (8.13) the coefficient A is independent of q. Summing Eq. (8.13) over the surface modes one obtains

$$\operatorname{div}\mathbf{U} = \sum_q AJ_0(qr)\exp(\lambda t) \sim \int_0^{q_0}[q\exp(t\chi(q_{R\sigma}^2-q^2))]\,J_0(qr)\,dq.$$

The function in square brackets reaches a maximum at $q = q_{\max} = (2\chi t)^{-1/2}$ (Fig. 39) and $\operatorname{div}\mathbf{U} \sim J_0(q_{\max}r)$. Using $t = \lambda(q_{\max})^{-1}$, one finds

$$q_{\max} \equiv q_{R\sigma}, \quad \lambda_{\max} \equiv \chi q_{R\sigma}^2. \quad (8.29)$$

The ring structure with $q = q_{\max}$ and $\lambda = \lambda_{\max}$, given by Eq. (8.29) is selected at $\sigma \gg R$. Note that in the case $\sigma \gg R$ one should not expect the formation of distinct and well developed surface periodic structures as in the case $\sigma \ll R$. Most probable in the case $\sigma \gg R$ are quasilocal structures with two or three oscillations. Putting in Eq. (8.26) $\lambda = 0$ one obtains the equation determining the critical temperature T_{cr} of excitation of the qth harmonic in CDTI

$$\exp(-w_{cr})\left(Q+\frac{S(1-\beta)}{w_{cr}}\right)/w_{cr} = \chi\Gamma q(1-\beta); \quad (8.30)$$

where $w_{cr} \equiv \dfrac{W_0(0)}{kT_{cr}}$, and Q and S are determined by Eqs. (8.22) and (8.10a). Thus, it follows from the consideration of this section that when the temperature of the medium exceeds the critical value $T_0(0) > T_{cr}(q)$ the CDTI develops in the subsurface layer (i.e., $\lambda(q) > 0$). As a result, the coupled concentric rings of temperature (8.14) of the displacement vector (8.18 - 8.21) and of the deformation (8.13) are formed. The period of these structures, i.e., the distance between the adjacent circles, is $d \cong 7/q_{\max}$.

As is seen from Eq. (8.7), the fields $\operatorname{div}\mathbf{U}$ and T_1 modulate the crystallization rate so that the ring periodic surface structures of crystalline and amorphous phases are formed as a result of CDTI (Fig. 2). These structures penetrate into the bulk by a distance δ^{-1}, $\kappa_{l,t}^{-1}$.

Similar to Sec. 2.5, the formation of the radial rings (see Fig. 2) described by the Eqs. (2.41), and ray structures (Fig. 2) described by Eq. (4.18) is also possible.

We estimate the period of the structures in the case of amorphous Si at the melting temperature $T = T_{\max} =$ 1400 K. The characteristic values of the parameters for

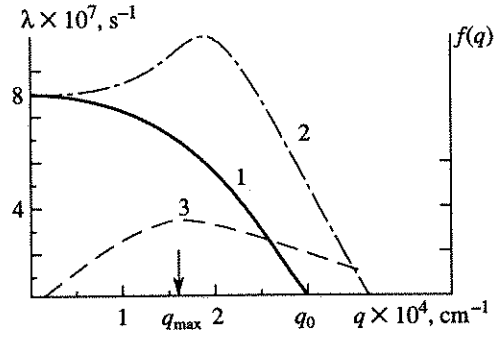

Fig. 39. *Dependence of the CDTI growth rate on the wavenumber q (calculation according to Eqs. (8.26) and (8.27a)). 1 – the growth rate at σ ≫ R, 2 – at σ ≪ R (schematically). 3 – the function qexp(tχ(q²_Rσ − q²) selecting the structure with q_max and λ_max (see Eq. (8.29).*

α–Si are $\tau_0 = 3.2 \times 10^{-15}$ s, $E_c = 10^3$ J·cm^{-3} [148], $|\theta| \approx$ 10 eV, $c_v \approx 2$ J·cm^{-3}·degree^{-1}, $\rho = 2.3$ g·cm^{-3}, $\beta = 0.2$, $K = 10^{12}$ erg·cm^{-3}, $\alpha = 10^{-6}$ K^{-1}, $\chi = 0.1$ cm^2·s^{-1}. At these values in Eq. (8.22) $Q = 3 \times 10^{14}$ s^{-1}, and $R = 4 \times 10^6$ s^{-1}, at $W_0 = 1.9$ eV. (The value of activation energy depends on the character of amorphization and varies in the limits 1.8 - 2.3 eV [138, 149, 150].)

From Eq. (8.10a) one has also $S = 4.2 \times 10^{17}$ s^{-1}, and $\sigma = 3.3 \times 10^8$ s$^{-1} \gg R$. Thus, under these conditions one can expect not the formation of well-developed periodic surface structures, but rather structures with only a few oscillations on the surface of a semi-infinite α–Si. At $\sigma = 3.3 \times 10^8$ s^{-1}, from Eq. (8.29) for these structures we have $\Gamma = 10^5$ cm^{-1}, so that the period $d \approx 3$ μm, and the growth rate $\lambda \sim 7 \times 10^7$ s^{-1} ($\tau^{-1} = 6 \times 10^7$ s^{-1}).

Let us evaluate the critical temperature. From Eq. (8.30) we have $w_{cr} = 16$ at $W = 1.9$ eV, $q = 2 \times 10^4$ cm^{-1} and $\Gamma = 10^5$ cm^{-1}. At the same values of parameters at $T = 1400$ K the value $w = W / kT = 15.5 < w_{cr}$, i.e., under these conditions the critical condition (8.30) can be fulfilled.

The formation of the "star"-like radial-ring structures was observed in experiments carried out with α–Ge film of a thickness 0.5 μm deposited on Si substrate with SiO_2 layer of a thickness 1 μm. This sandwich-type structure was irradiated by the laser pulses with $\tau_p = 30$ ns, $\lambda = 0.51$ μm, and energy density 0.5 J·cm^{-2} [144]. After irradiation with a single pulse, several "star" structures of surface relief modulation were recorded, similar to that shown in Fig. 38, with chaotic distribution of centers of the "stars." This circumstance can be attributed to the presence of either enhanced optical absorption, or of lowered activation energy (or both) on the surface of centers due to, for example, local deformation.

The CDTI in a film-on-substrate structure can be modeled by a CDTI in a semi-infinite medium, but in this case one must take into account the modified properties of the top layers. This system seems to be better described in the framework of the theory of CDTI in films which is considered below.

8.2. Amorphous Films

The problem of laser recrystallization of amorphous semiconductor films is important for microelectronics [147]. The formation of periodic structures is often observed [147] when carrying out laser induced recrystallization using either cw or pulsed laser radiation. One of the possible mechanisms of their formation is CDTI, considered in Sec. 8.1 for the case of the surface of amorphous media.

In this section we generalize the mechanism of CDTI for the case of amorphous films. The physical mechanism of CDTI in a film is essentially the same as that on the surface, but now the bending or the longitudinal deformation of the film [76] plays the main role, instead of the surface deformation. We shall confine ourselves here to the case of bending deformations only.

Let us consider a thin film of a thickness h of amorphous material illuminated by laser light. We assume the case of strong absorption, so that the film is optically thick. Let $a = a(x, y)$ be the local relative volume of amorphous phase, defined in Sec. 8.1. The variable a obeys the activation kinetic equation (8.1).

The equation for T in the film is given by

$$\partial T/\partial t = \chi \Delta T - \mu (T - T_s) + (E_c a/\tau_0 c_v) \times \exp(-(W + \theta \operatorname{div} \mathbf{U})/kT) + c\gamma |E|^2 (1 - R)/2\pi c_v, \quad (8.31)$$

where μ is the phenomenological constant accounting for thermal conductivity into the substrate with the temperature T_s, the rest of the parameters being the same as in Eq. (8.2).

We shall approximate the bending deformations in the considered structure by the equation for the unsupported film, accounting for the interface by introducing the longitudinal stress

$$\frac{\partial^2 \zeta}{\partial t^2} = -c^2 l_0^2 \Delta^2 \zeta + c_\parallel^2 \Delta \zeta - (K\alpha\nu/\rho h) \int_{-h/2}^{h/2} z \Delta T dz. \quad (8.32)$$

Here $c_\parallel^2 = \sigma_\parallel / \rho$, $\sigma_\parallel$ is the stress along the film, occurring due to the difference of the thermal expansion coefficients of the film (α) and the substrate; $l_0^2 = h^2/12$, $\nu = (1 - 2\sigma)/(1 - \sigma)$.

The bending deformation is linked with the strain by Eq. (4.32), as usual. The system of Eqs. (8.1), (8.31), (8.32), and (4.32) is the closed system describing CDTI in the amorphous film.

In a linear regime of CDTI we represent the problem variables in the form of the sum of spatially uniform zero-order solutions and spatially nonuniform first order perturbation

$$a = a_0 + a_1, \quad T = T_0 + T_1, \quad \zeta = \zeta_0 + \zeta_1, \quad \operatorname{div} \mathbf{U} = \xi_0 + \xi_1.$$

Linearizing Eqs. (8.1) and (8.31) with respect to perturbations, we obtain the zero-order equations for spatially uniform variables

$$da_0/dt = -a_0/\tau;\ \tau^{-1} = \tau_0^{-1}\exp(-W_0/kT_0),$$
$$\partial T_0/\partial t = \chi\partial^2 T_0/\partial z^2 - \mu(T_0 - T_s) + E_c a_0/\tau c_v + c\gamma|E|^2(1-R)/2\pi c_v, \quad (8.33)$$

where $W_0 = W + \theta \mathrm{div}\, U_0$, and with proper account for Eq. (4.32), the first-order equations for spatially nonuniform variables

$$\partial T_1/\partial t = \chi\Delta T_1 - \mu T_1 + E_c a_1/\tau c_v + (E_c a_0/\tau c_v)(W_0 T_1/kT_0^2 - \theta\xi_1/kT_0),$$
$$da_1/dt = -a_1/\tau + (a_0/\tau)(\theta\xi_1/kT_0 - W_0 T_1/kT_0^2). \quad (8.34)$$

If one neglects the thermal conductivity ($\chi = 0$, $\mu = 0$), then from Eq. (8.34) one obtains the energy conservation law

$$\frac{\partial}{\partial t}(E_c a_1 + c_v T_1) = 0.$$

Under the condition $\lambda\tau \gg 1$ one can neglect the term $\sim a_1$ in the second equation in Eqs. (8.34). The perturbed crystallization rate is governed by the equation

$$da_1/dt = (a_0/\tau)(\theta\xi_1/kT_0 - W_0 T_1/kT_0^2). \quad (8.35)$$

We take into account that the fourth term in the right-hand side of the first of Eqs. (8.34) is by a factor of $W_0 T_1 a_0 / k a_1 T_0^2 \sim W_0/kT_0 \gg 1$ larger than the third one, proportional to a_1, which we shall neglect. From Eqs. (8.34) and (8.32) we obtain the closed system of equations describing CDTI in the film

$$\partial T_1/\partial t = \chi\Delta T_1 + gz\nu\Delta\zeta + (\sigma - \mu)T_1,$$
$$\frac{\partial^2\zeta_1}{\partial t^2} = -c^2 l_0^2\Delta^2\zeta_1 + c_\parallel^2\Delta\zeta_1 - (K\alpha\nu/\rho h)\int_{-h/2}^{h/2} z\Delta T_1 dz, \quad (8.36)$$

where

$$g = -E_c a_0\theta/\tau c_v kT_0;\ g > 0,$$
$$\sigma = (E_c/c_v)\, a_0 \left(\frac{W_0}{kT_0^2}\right)\frac{\exp(-W_0/kT_0)}{\tau_0}.$$

Developing the solution of the system (8.36) in the form $T_1, \zeta_1 \sim \exp(\lambda t + iqx)$ we find (under the condition $\lambda^2 \ll c^2 l_0^2 q^4 + c_\parallel^2 q^2$) the expression for the growth rate

$$\lambda = -\chi q^2 + \sigma - \mu + Rq^2/(1 + c^2 l_0^2 q^2/c_\parallel^2), \quad (8.37)$$

where the externally controlled parameter R, determining the transition to the spatially nonuniform state, depends on the mean temperature

$$R = R(T_0) = \nu^2 a_0 \left(\frac{K}{\rho c_\parallel^2}\right)\left(\frac{\alpha E}{c_v}\right)\left(\frac{\exp(-W_0/kT_0)}{\tau_0}\right)\left(\frac{|\theta|}{kT_0}\right). \quad (8.38)$$

This describes the coupling through the deformation potential θ between the elastic properties of the medium (described by the elasticity modules (K)) and crystallization properties of the amorphous medium (described by latent crystallization heat E_c). Parameter σ describes the usual spatially uniform explosive crystallization.

The dependence $\lambda = \lambda(q)$ reaches the maximum value $\lambda = \lambda_{max}$ at $q = q_{max}$:

$$q_{max} = \frac{1}{l_0}\frac{c_\parallel}{c}\left[\left(\frac{Rl_0^2}{\chi}\right)^{1/2} - 1\right]^{1/2},$$
$$\lambda_{max} = \sigma - \mu + \frac{c_\parallel^2}{c^2}(R^{1/2} - \chi^{1/2}/l_0)^2 = \sigma - \mu + \lambda_R. \quad (8.39)$$

It follows from Eq. (8.39) that the maximum of $\lambda = \lambda(q)$ exists under the condition

$$R > \chi/l_0^2. \quad (8.40)$$

If an extra condition $\lambda_{max} > 0$ is imposed (to fulfil the latter it is sufficient to have $\sigma = \sigma(T_0) > \mu$) the CDTI sets in the film, accompanied by the formation of one-dimensional coupled gratings of temperature T_1 and bending deformation ζ with the period

$$d = 2\pi/q_{max} = 2\pi\frac{c}{c_\parallel}l_0[(Rl_0^2/\chi)^{1/2} - 1]^{-1/2}. \quad (8.41)$$

Due to Eq.(8.35) these gratings modulate the crystallization rate, so that the grating of alternating amorphous and crystalline phases must be formed with the period given by Eq. (8.41).

Under the condition

$$R < \chi/l_0^2$$

the maximum of the dependence $\lambda = \lambda(q)$ is achieved at $q = 0$, which is equal to $\lambda = \lambda_{max} = \sigma - \mu$. Under the extra condition $\sigma > \mu$, there develops the thermal explosive crystallization ($\lambda > 0$), but the periodic structures are not formed in this case.

Let us do some numerical estimations. In the case of CdS, $K = 5\times10^{11}$ erg·cm^{-3}, $\rho = 5$ g·cm^{-3}, $\alpha = 5\times10^{-6}$ K^{-1}, $c_v = 1.6$ J·cm^{-3}, $\chi = 0.1$ cm^2·s^{-1}. Using also $E_c = 4\times10^3$ J·cm^{-3}, $W = 1.3$ eV [149], $\theta = 5$ eV, $\tau_0 = 3\times10^{-15}$ s [152], $c/c_\parallel \sim 5$, $\nu = 1$, $a_0 = 1$, at $T = 10^3$ K the control parameter is $R = 1.3\times10^9$ s^{-1}, and at $h = 2$ μm we have $Rl_0^2/\chi = 70$, i.e., the critical condition of CDTI (8.40) can be fulfilled at the temperature $T \sim 10^3$ K. From Eq. (8.41) at the same values of the parameters one finds the grating period to be

$d \sim 7$ μm. The critical temperature, found from Eq. (8.40) is $T \sim 5 \times 10^2$ K.

Let us estimate now the time of grating formation, using Eqs. (8.37) and (8.39): with the values of parameters used above we have $\sigma \sim 10^9$ s^{-1}, $R \sim 10^9$ s^{-1} in these formulas and $\lambda_R \sim 10^7$ s$^{-1} \ll \sigma$ in Eq. (8.11). Thus, the periodic structure appears only in the region $|\sigma - \mu| < \lambda_R$. Hence, in the case of bell-shaped temperature distribution $T_0 = T_0(r)$ it appears in the ring region $r_{\min} < r < r_{\max}$.

Note in conclusion of this section that the surface of the film, as well as that of the semi-infinite sample (Sec. 8.1) must be periodically undulated, if it becomes recrystallized under the conditions of CDTI. The surface undulations in explosive crystallization are in fact observed (see Ref. [153]). Other instabilities in crystallization and solidification processes are reviewed in Refs. [154, 155].

9. CONCLUSION

In this work, on the basis of the DD model of a solid we studied the hierarchy of the processes of laser-induced defect generation and subsequent transformations of defect fields, leading to formation of the localized and periodic defects structures on strongly absorbing surfaces of solids and in films.

Strong action of the laser radiation greatly enhances the rate of defect generation and leads to creation of dense fields of point defects in the subsurface layers of materials due to the heating, deformation of medium and electronic excitation. Other processes induced at the surface by other types of energy beams (chemical reactions, implantation, particle irradiation) also yield very high concentrations of point defects. The self-consistent medium deformation, induced by point defects, ensures the appearance of positive feedback in the processes of point defect generation and deformation-induced drift and leads to occurrence of the GDDI.

The threshold of onset of the GDDI of point defect fields n_{cr1} is the first threshold in the considered hierarchy of defect field transformations. It marks the beginning of formation of either extended defects or periodic point defect pileups. With further energy beam-induced generation and corresponding increase of the number of point defects, the second threshold n_{cr2} is reached after exceeding of which the periodic structures of extended defects are formed. We believe that this second threshold (or the third, close to it, threshold n_{cr3}) marks also the onset of the self-consistent deformation-induced local fusion of extended defects, i.e., the formation of cracks, and thus damage of the material. The mechanism of accumulative laser damage, developed here with the use of this assumption, yields results which are in good agreement with the experimental data on laser damage of semiconductors by trains of laser pulses.

The exceeding of the first threshold n_{cr1} was shown also to have practically important manifestations (catastrophic degradation of optoelectronic devices, nonuniform surface melting of semiconductors, formation of periodic subboundaries structures and others). The predictions of the GDDI theory as to the periods, orientations and the time of development of the surface structures are in good agreement with experimental results.

The interpretation of peculiarities of laser-induced surface grating formation in covalent semiconductors from the viewpoint of DDI enabled us to draw conclusions about the possibility of controlling the directions of diffusion and deformation-induced vacancy and interstitial surface fluxes with the help of a linearly polarized strong laser beam. We believe that similar control of the direction of diffusion and deformation-induced fluxes of electron-hole pairs is also possible in the case of EDTI. Thus the control of the orientation of the surface relief gratings formed due to the EDTI seems to be possible either due to laser excitation and breaking of selective direction covalent bonds or due to intense laser field-induced anisotropy of the electron relaxation times.

Interpretation of laser-induced morphological changes from the viewpoint of GDDI leads us to a conclusion about the mutual influence of two different instabilities: the interference instability of surface relief and GDDI. In light of these results, the possibility of entrainment of point defects by spatially periodic surface light fields, arising spontaneously under the conditions of surface ripple formation, appears very promising. These questions need further theoretical and experimental investigation.

The results of the present studies of the periodic DD-structure formation enable us to make a conclusion about the crucial role of surface in determining the character of the generated structures.

The boundary conditions for deformation and diffusion fields at the surface (or effective form of the basic equations in the solid films) ensure the occurrence of a maximum in the dependence of the instability growth rates on the grating wavenumber, thus leading to generation of periodic defect structures. In the bulk case this dependence is monotonous, which results in formation of quasilocalized DD structures.

The initial state of the surface and subsurface layers turns out to be of great importance for the effects of GDDI studied above.

First, the rate of laser-induced defect production in semiconductors and the subsurface layer, in which the intensive defect generation multiplication takes place, is determined essentially by the initial defectiveness of the material. Second, the initial extended defects lower the thresholds of GDDI by their deformation fields (or, possibly, by their electric fields), thus initiating the onset of instabilities and formation of additional extended defects in their vicinity. Thus, the resulting effects, such as degradation of optoelectronic devices, nonuniform melting

of the surface, cumulative damage and others, viewed here as manifestations of GDDI, essentially depend on the initial defectiveness of the subsurface layers.

Apart from endothermal GDDI we considered also exothermal GDDI in amorphous media. Another possible type of exothermal GDDI considered recently is the recombinational DDI developing, by analogy with CDTI considered in Sec. 8, due to heat extraction during recombination of defects [156].

The GDDI considered in this review belong to the class of nonresonant laser-induced processes. The frequency of laser radiation may be varied in wide limits without changing essentially the observed effects, and no coherence of radiation is needed to induce GDDI. Recently the class of laser-induced resonance instabilities and phase transitions in quantum electronics systems with discrete energy levels was also investigated [151].

We believe that the studies of GDDI, as compared with the state-of-the-art in interference instabilities of the surface relief, are now only at the initial stage. Many conclusions made in this work should be viewed at present as only hypotheses. We hope that this review will stimulate further progress in research in this field of laser physics.

ACKNOWLEDGMENT

The author is grateful to professors S.A. Akhmanov, A.M. Bonch-Bruevich, M.N. Libenson, Yu.V. Kapaev, P.K. Kashkarov, L.V. Keldysh, N.I. Koroteev, L.D. Laude, B.S. Luk'yanchuk, A.A. Manenkov, V.Ya. Panchenko and H. van-Driel and also to Drs. A.F. Banishev, S.V. Govorkov, I.L. Shumay, and A.A. Soumbatov for fruitful discussions in the course of the present work.

REFERENCES

1. Ed. Laude, L.D., 1983, *Cohesive Properties of Semiconductors under Laser Irradiation* (Hague, Boston, Lanatster: Martinus Nijhoff Publ.).
2. Ueda, O., 1988, *Electrochem. Soc.*, **145**, 11.
3. Jones, S.C. *et al.*, 1989, Laser-Induced Material Modifications, *Opt. Eng.*, **28**, 1039.
4. Eds. Birman, J.L., Cummins, H.Z., and Kaplyanskii, A.A., 1988, *Laser Optics of Condensed Matter* (New York: Plenum Press).
5. Akhmanov, S.A., Koroteev, N.I., and Shumay, I.L., 1989, Nonlinear Optical Diagnostics of Laser Excited Semiconductor Surfaces. Laser Science and Technology, *An International Handbook*, **2**, Eds. Letokhov, V.S., Shank, C.V., Shen, Y.R., and Walter, H. (Chur, Switzerland: Harwood Academic Publ.).
6. Shank, C.V., Yen, R., and Hirlimann, C., 1983, *Phys. Rev. Lett.*, **50**, 454; *Phys. Rev. Lett.*, **51**, 900.
7. Tom, H.W.K., Aumiller, G.D., and Brito-Cruz, C.H., 1983, *Phys. Rev. Lett.*, **60**, 1438.
8. Schröder, T., Rudolph, W., Govorkov, S.V., *et al.*, 1990, *Appl. Phys. A*, **51**, 49.
9. Sokolowskii-Tinten, K., Schulz, H., Bialkowskii, J., *et al.*, 1991, *Appl. Phys. A*, **53**, 227.
10. Bertolotti, M., Vitali, G., Zammit, U., *et al.*, 1982, *Laser and Electron-Beam Interactions with Solids*, Eds. Appleton, B.R. and Celler, G.K., **4**, 203.
11. Celler, G.K., 1983, *J. Cryst. Growth*, **63**, 429.
12. Givargizov, E.I. and Limanov, A.B., 1988, *Microelectronic Engineering*, **8**, 273.
13. Bauerly, D., 1986, Chemical Processing with Lasers, *Springer Ser. Mater. Sci.*, **1** (Berlin: Springer-Verlag).
14. Matare, H.F., 1971, *Defect Electronics in Semiconductors* (New York: Wiley).
15. Holloman, J.H., Mauer, R., and Seitz, F., *Imperfections in Nearly Perfect Crystals*, Ed. Schokly, W. (New York: Wiley).
16. Boiko, V.I., Luk'yanchuk, B.S., and Tzharev, E.P., 1991, *Proc. General Physics Institute of the USSR Academy of Sciences*, **30**, 6.
17. Bolling, G.F. and Fainstein, D., 1972, *Philos. Mag. A*, **25**, 45.
18. Van Siclen and Wolfer, W.G., 1991, *Phys. Rev. A*, **43**, 5344.
19. Palatnik, L.S., Cheremskoi, P.G., and Fuks, M.Ya., 1982, *Voids in Films* (Moscow: Energoizdat) (in Russian).
20. Singh, B.N., Leffers, T., and Horsewell, A., 1986, *Philos. Mag. A*, **53**, 233.
21. *Materials Research Society Proceedings*, 1986, **52**.
22. Young, J.F., Preston, J.S., Van Driel, H., *et al.*, 1983, *Phys. Rev. B*, **27**, 1141; 1155.
23. Siegman, A.E. and Fauchet, P.M., 1986, *IEEE J. Quantum Electron.*, **QE-4**, 1384.
24. Akhmanov, S.A., Emel'yanov, V.I., and Koroteev, N.I., 1990, Interaction of Strong Laser Radiation with Solids and Nonlinear Optical Diagnostics of Surfaces, *Teubner Texte zur Physik*, **24** (Leipzig: Teubner).
25. Akhmanov, S.A., Emel'yanov, V.I., Koroteev, N.I., and Seminogov, V.N., 1985, *Sov. Phys. Usp.*, **28**, 1084.
26. Emel'yanov, V.I. and Seminogov, V.N., 1988, Topics on Science and Technology, *Series "Physical Fundamentals of Laser and Particle Beam Technology,"* **1**, 118 (Moscow: VINITI); *ibid.*, 1989, **3**, 57 (in Russian).
27. Emel'yanov, V.I., 1985, *Preprint of the Physics Faculty of Moscow State University*, no. 5, Moscow, USSR.
28. Emel'yanov, V.I., 1989, *Nonlinear Waves* (Moscow: Nauka) (in Russian).
29. Emel'yanov, V.I., 1988, Instabilities and Phase Transitions with Formation of Ordered Surface Structures under the Action of External Energy Beams, *Proc. Intern. Symp. on Selected Topics in Statistical Mechanics*, Joint Institute for Nuclear Research, D 17-88-95, Dubna, USSR, 119.
30. Eshelby, J.D., 1956, The Continuum Theory of Lattice Defects, *Solid State Physics*, **3** (New York: Academic Press).
31. Kosevich, A.M., 1981, *Physical Mechanics of Real Crystals* (Kiev: Naukova Dumka).
32. Ridley, B.K., 1982, *Quantum Processes in Semiconductors* (Oxford: Clarendon Press).

33. Nicolis, G. and Prigogine, I., 1977, *Self-Organization in Nonequilibrium Systems* (New York: Wiley).
34. Haken, H., 1978, *Synergetics* (Berlin: Springer-Verlag).
35. Vasil'ev, V.A., Romanovskii, Yu.M., and Yakhno, V.G., 1987, *Autowave Processes* (Moscow: Nauka) (in Russian).
36. Kerner, B.S. and Osipov, V.V., 1991, *Autosolitons* (Moscow: Nauka) (in Russian).
37. Bugaev, A.A. and Klochkov, A.V., 1984, *Sov. Phys. Sol. State*, **26**, 2100.
38. Baskin, B.L., Polyakov, A.A., Trukhin, V.N., *et al.*, 1985, *Sov. Tekh. Phys. Lett.*, **11**, 517.
39. Merkle, K.L., Uebbing, R.H., Baumgart, H., *et al.*, 1982, *Laser and Electron Beam Interactions with Solids*, Eds. Appleton, B.R. and Celler, G.K. (New York: North Holland).
40. Tom, H.W., Aumiller, G.D., and Brito-Cruz, C.H., 1988, *IEEE J. Quantum Electron.*, **24**, 48.
41. Emel'yanov, V.I. and Uvarova, I.F., 1986, *Bull. Acad. Sci. USSR, Ser. Phys.*, **50**, 1214.
42. Emel'yanov, V.I. and Uvarova, I.F., 1988, *Sov. Phys. JETP*, **67**, 1662.
43. Kopaev, V.V., Kopaev, Yu.V., and Molotkov, C.N., 1983, *Microelectronics*, **12**, 499.
44. Kopaev, Yu.V., 1985, *Zh. Tekh. Fiz.*, **30**, 1328.
45. Kash, J.A., Tsang, J.C., and Hvam, J.M., 1985, *Phys. Rev. Lett.*, **54**, 2151.
46. Smirl, A.L., 1984, *Semiconductors Probed by Ultrafast Laser Spectroscopy*, Ed. Alfano, R.R., **1**, 198, (Orlando-Tokio: Academic Press).
47. Govorkov, S.V., Emel'yanov, V.I., and Shumay, I.L., 1992, *Laser Physics*, **2**, 79.
48. Spain, I.L., Hu, J.Z., Menoni, C.S., *et al.*, 1984, *J. Phys. (Paris)*, **45**, Coll. C8, Suppl. 11, C8-407.
49. Kopaev, Yu.V., Menaylenko, V.V., and Molotkov, S.N., 1985, *Sov. Solid State Physics*, **27**, 3288.
50. Biswas, R. and Ambegaokar, V., 1982, *Phys. Rev. B.*, **26**, 1980.
51. Wang, J.K. *et al.*, 1990, *Ultrafast Phenomena VII*, Eds. Harris, C.B., Ippen, E.P., Mourou, G.A., and Zewail, A.Q.H., *Springer Series on Chem. Phys.*, **53**, 365 (Berlin: Springer-Verlag).
52. Wood, R.F. and Jelison, G.E., 1984, *Semiconductors and Semimetals*, Ed. Wood, R.F., White, C.W., and Young, R.T., **23**, 166 (Orlando-Tokyo: Academic Press).
53. Celler, G.K., 1984, Modification of Silicon Properties with Lasers, Electron Beams and Incoherent Light CRC, *Crit. Rev. Solid State and Mater. Sci.*, **2**, 193.
54. Karyagin, S.N., Kashkarov, P.K., Kiselev, V.F., and Petrov, A.V., 1984, *Surf. Sci.*, **146**, 1852.
55. Kashkarov, P.K. and Petrov, A.V., 1985, *Fiz. Tekh. Poluprovodn.*, **19**, 234.
56. Chechenin, N.G., Burdel, K.K., Zenkov, Yu.V., *et al.*, 1986, *Nucl. Instrum. Methods Phys. Res., Sect. B*, **13**, 503.
57. Kashkarov, P.K. and Kiselev, V.F., 1986, *Izv. Akad. Nauk SSSR, Ser. Fiz.*, **50**, 435.
58. Baeri, P.J., 1985, *Luminescence*, **30**, 409.
59. Corbett, J.W. and Borgoin, J.C., 1975, *Point Defects in Solids, Semiconductors and Molecular Crystals*, Eds. Crawford, J.H. and Slifkin, K.M., **2** (New York: Plenum Press).
60. Bourgoin, J.M. and Lanno, M., 1983, *Point Defects in Semiconductors II. Experimental Aspects* (Berlin: Springer-Verlag).
61. Klinger, M.I., Lushchik, Ch.B., Maskovets, T.V., *et al.*, 1985, *Usp. Fiz. Nauk*, **147**, 523.
62. Itoh, N., 1983, *Semiconductors and Insulators*, **5**, 165.
63. Emel'yanov, V.I. and Kashkarov, P.K., 1987, Electron-Deformation-Thermal Mechanism of Defect Generation in Semiconductors under Pulsed Laser Action, *Preprint of Physics Faculty of Moscow State University*, no. 16; 1990, *Poverkhnost*, no. 2, 77.
64. Khait, Yu.L., Salzman, J., and Beserman, R., 1989, *Appl. Phys. Lett.*, **55**, 1170.
65. Moin, M.D., 1984, *Fiz. Tverd. Tela*, **26**, 2742.
66. Appolonov, V.V., Barchukov, A.I., Karlov, N.V., *et al.*, 1975, *Kvantovaya Elektronika*, **2**, 380.
67. Gauster, W.B., 1965, *Phys. Rev.*, **67**, 1035.
68. Gauster, W.B. and Habing, P.H., 1967, *Phys. Rev. Lett.*, **18**, 1058.
69. Rotshild, R., Arnone, C., and Ehrlich, D.J., 1987, *J. Mater. Res.*, **2**, 244.
70. Van Vechten, J.A., 1982, *J. Appl. Phys.*, **21**, 125.
71. Emel'yanov, V.I., Kashkarov, P.K., Chechenin, N.G., and Ditrikh, T., 1988, *Fiz. Tverd. Tela*, **30**, 2259.
72. Zenkov, Yu.V., 1987, *PhD Thesis*, Moscow State University, Moscow, USSR.
73. Emel'yanov, V.I. and Kashkarov, P.K., 1992, *Appl. Phys. A* (in press).
74. Emel'yanov, V.I., Makin, V.S., and Uvarova, I.F., 1990, *Fiz. Khim. Obrab. Mater.*, **2**, 12.
75. Emel'yanov, V.I. and Uvarova, I.F., 1989, *Metallofizika*, **11**, 101.
76. Landau, L.D. and Lifshits, E.M., 1987, *Theory of Elasticity*, Ch. 3 (Moscow: Nauka) (in Russian).
77. Gusev, V.E., Kozlova, E.K., and Portnyagin, A.I., 1987, *Kvantovaya Elektronika*, **14**, 323.
78. Mogyorosi, P., Piglmayer, K., and Bauerly, D., 1989, *Surface Science*, **208**, 232.
79. Banishev, A.F., Emel'yanov, V.I., and Novikov, M.M., 1992, *Laser Physics*, **2**, 192.
80. Anisimiv, V.N. *et al.*, 1983, *Poverkhnost*, no. 7, 138.
81. Landolf-Bornstein, 1980, **49** (Berlin: Springer-Verlag).
82. Lanno, M. and Bourgoin, J., 1981, *Point Defects in Semiconductors. I. Theoretical Aspects* (Berlin: Springer-Verlag).
83. Smith, H.I., Geis, M.W., Thompson, C.V., and Atwater, H.A., 1983, *J. Cryst. Growth*, **63**, 527.
84. Geis, M.W. *et al.*, 1982, *J. Electrochem. Soc.*, **129**, 2812.
85. Geis, M.W. *et al.*, 1985, *Energy Beam-Pulse Interactions and Transient Thermal Processing*, Eds. Rozgonyi, G.A. and Shank, C.V., **35**, 575 (Amsterdam: North Holland).
86. Tillack, B. *et al.*, 1988, *Phys. Status Solidi A*, **94**, 871.

87. Pfeiffer, L. *et al.*, 1986, *Semiconductor on Insulator and Thin Film Transistor Technology*, Eds. Chiang, A., Geis, M.W., and Pfeiffer, L., **3**, 29 (Amsterdam: North Holland).
88. Geis, M.W., *et al.*, 1983, *J. Electrochem. Soc.*, **130**, 1178.
89. Emel'yanov, V.I. and Soumbatov, A.A., 1990, *Vestn. Mosk. Univ., Fiz.*, **6**, 69.
90. Emel'yanov, V.I. and Soumbatov, A.A., 1991, *Laser Physics*, **1**, 122.
91. Geis, M.W. *et al.*, 1986, *J. Appl. Phys.*, **60**, 1152.
92. Cline, H.E., 1983, *J. Appl. Phys.*, **54**, 2683.
93. Mertens, P.W., 1991, Zone Melting Recrystallization of Silicon Films on Amorphous Substrates for Silicon-on-Insulator Applications, *PhD Thesis*, Katholicke Universiteit Leuven, Belgie.
94. Wilson, I.H., 1982, *J. Appl. Phys.*, **53**, 1698.
95. Appleton, B.R., Holland, O.W., and Narayan, J., 1982, *Appl. Phys. Lett.*, **41**, 71.
96. Appleton, B.R., Holland, O.W., and Narayan, J., 1983, *J. Appl. Phys.*, **54**, 2295.
97. Chaplanov, A.M. and Tochintskii, E.I., 1984, *Thin Solid Films*, **116**, 117.
98. Holland, O.W., Appleton, B.R., and Narayan, J., 1983, *J. Appl. Phys.*, **54**, 2295.
99. Chen, S., Lee, S.T., Braunstein, G., and Tan, T.Y., 1989, *Appl. Phys. Lett.*, **55**, 194.
100. Hirth, J. and Lote, I., 1972, *The Theory of Dislocations* (Moscow: Mir) (in Russian).
101. Emel'yanov, V.I. and Volodin B.L., 1990, *Sov. J. Quantum Electron.*, **17**, 648.
102. Volodin, B.L. and Emel'yanov, V.I., 1991, *Izv. Akad. Nauk SSSR, Ser. Fiz.*, **55**, 1274.
103. Sclosser, H. and Ferrante, J., 1989, *Condens. Matter*, **1**, 2727.
104. Chen, S., Lee, S.T., Braunstein, G., and Tan, T.Y., 1989, *Phys. Lett.*, **55**, 194.
105. Singh, B.N., Leffers, T., and Horsewell, A., 1986, *Philos. Mag. A*, **53**, 233.
106. Muncie, J.W., Eyre, B.L., and English, C.A., 1987, *Philos. Mag. A*, **52**, 309; *ibid.*, **56**, 453.
107. Hajdu, C., Paszti, F., Lovas, I., and Fried, M., 1990, *Phys. Rev. B*, **41**, 3920.
108. Proc. Intern. Conf. SELCO-87, 1987, Moscow; 1988, *Kvantovaya Elektronika*, **15**, no. 7).
109. Mizuishi, K. *et al.*, 1979, *J. Appl. Phys.*, **50**, 6668.
110. Strekalov, V., 1989, *Izv. Vyssh. Uchebn. Zaved., Fiz.*, **32**, 5.
111. Beister, G. *et al.*, 1988, *Kvantovaya Elektronika*, **15**, 2295.
112. Von Allmen, M.F., Luthy, W., and Affolter, K., 1978, *Appl. Phys. Lett.*, **33**, 824.
113. Celler, G.K., Robinson, Mc.D., Timble, L.E., and Lischner, D.J., 1983, *Appl. Phys. Lett.*, **43**, 868.
114. Fattakhov, Ya.V. and Khaibullin, I.B., 1988, *Pis'ma Zh. Tekh. Fiz.*, **14**, 1474.
115. Lee, C.S., Koumvakalis, N., and Bass, M.J., 1983, *Appl. Phys.*, **54**, 5727; 1983, *Opt. Eng.*, **22**, 419.
116. Tomas, S.J., Harrison, F.F., and Figueira, J.F., 1982, *Appl. Phys. Lett.*, **40**, 200.
117. Ursu, Z.I., Prokhorov, A.M., Konov, V.I., *et al.*, 1984, *Appl. Phys. A*, **34**, 133.
118. Veiko, V.P., Kotov, G.A., Smirnov, V.N., *et al.*, 1981, *Kvantovaya Elektronika*, **8**, 2196.
119. Fauchet, P.M., 1983, *Phys. Lett. A*, **93**, 155.
120. Manenkov, A.A. and Nechitaylo, V.S., 1990, *Izv. Akad. Nauk SSSR, Ser. Fiz.*, **54**, 2356.
121. Bass, M. and Barret, H.H., 1971, Laser-Induced Damage in Optical Materials, *NBS Special Publication*, **356**, 76.
122. Lee, C.S., Koumvakalis, N., and Bass, M., 1982, *Appl. Phys. Lett.*, **41**, 625.
123. Musal, H.M., 1979, *NBS Special Publication*, **568**, 159.
124. Jones, S.C., Braunlich, P.F., Casper, R.T., and Kelly, P., 1990, *Nucl. Instrum. Methods Phys. Res., Sect. B*, **46**, 231.
125. Volodin, B.L. and Emel'yanov, V.I., 1991, *Thesis of ICONO'91*, **130**, Leningrad, USSR.
126. Emel'yanov, V.I., Shlykov, Yu.G., and Volodin, B.L., 1992, *Proc. ICONO'91*; *Proc. SPIE* (in press).
127. Bagratashvili, V.N., Banishev, A.F., Emel'yanov, V.I., *et al.*, 1991, *Appl. Phys. A*, **52**, 438.
128. Weaver, C., 1971, *Diffusion in Metallic Films in Physics of Thin Films*, Eds. Francobe, M.H. and Hoffman, R.W., **6** (New York: Academic Press).
129. Pilecki, S., 1977, *Archive of Mechanics*, **29**, 505.
130. Walgraef, D. and Aifantis, E.C., 1986, *Int. J. Eng. Sci.*, **23**, 1789.
131. Schiller, C. and Walgraef, D., *Acta Metall.*, **36**, 563.
132. Neumann, P., 1987, *Phys. Scr.*, **19**, 537.
133. Tabata, T. *et al.*, 1983, *Philos. Mag. A*, **47**, 841.
134. Banishev, A.F., Volodin, B.L., and Emel'yanov, V.I., 1990, *Fiz. Tverd. Tela*, **32**, 2529.
135. Demchuk, A.V., Danilovich, N.I., and Labunova, V.A., 1985, *Poverkhnost'*, no. 11, 26.
136. Hunt, R.A. and Gale, B., 1972, *J. Appl. Phys. D*, **5**, 359.
137. Frohlich, H., 1962, *Polarons and Excitons*, Eds. Kuper, C.G. and Whitefield, G.D., Part 1 (Edinburgh: Wagner, Oliver, and Boyd).
138. Cesari, C., Nihoul, G., Marfaing, J., *et al.*, 1985, *Surface Science*, **162**, 724.
139. Gotz, G., 1986, *Appl. Phys. A*, **40**, 29.
140. Geiler, H.D., Glaser, E.G., Gotz, G., and Wagner, M., 1986, *J. Appl. Phys.*, **59**, 3091.
141. Andrew, R. and Wautelet, M., 1983, *J. Phys. (Paris)*, Colloq. C5, suppl. 10, 44.
142. Kanemitsu, Yo., Tanaka, Yu., and Kuroda, H., 1985, *Jpn. J. Appl. Phys.*, **24**, 1959; *Appl. Phys. Lett.*, 1985, **47**, 939.
143. Kim, D.K., Shah, R.R., and Von der Linde, D., 1982, *Laser and Electron Beam Interactions with Solids*, Eds. Appleton, B.R. and Celler, G.K. (Amsterdam: North Holland), 85.
144. Emel'yanov, V.I. and Soumbatov, A.A., 1988, *Poverkhnost*, no. 7, 122.
145. Abdullaev, A.Yu., Govorkov, S.V., Koroteev, N.I., *et al.*, 1986, *Pis'ma Zh. Tekh. Fiz.*, **12**, 1100.
146. Arutyunov, E.N., Vasil'ev, A.N., Koval'chuk, Yu.N., *et al.*, 1984, *Pis'ma Zh. Tekh. Fiz.*, **10**, 1281.
147. Aleksandrov, L.N., *Kinetics of Crystallization and Recrystallization of Semiconductor Films* (Novosibirsk: Nauka) (in Russian).
148. Heinig, K.H. and Geiler, H.D., 1985, *Phys. Status Solidi A*, **92**, 421.

149. Bourgoin, J.C. and Asomosa, R., 1983, *J. Phys. (Paris)*, Colloq. C5, suppl. 10, **44**, 175.
150. German, P.J., Paesler, M.A., and Zellama, K., 1983, in the book, cited in Ref. [1].
151. Andreev, A.L., Emel'yanov, V.I., Il'inskii, Yu.A., 1992, *Superradiance and Light-Induced Phase Transitions* (Bristol: Adam Hilger).
152. Heinig, K.H. and Geiler, H.D., 1986, *Phys. Status Solidi A*, **93**, 99.
153. Van Saarloos, W. and Weeks, J.D., 1984, *Physica*, **12D**, 279.
154. Sekerka, R.F., 1984, *Physica*, **12D**, 212.
155. Langer, J.S., 1980, *Rev. Mod. Phys.*, **52**, 1.
156. Mirzoev, F.H., Panchenko, V.Ya., and Shelepin, L.A., 1990, *Zh. Tekh. Fiz.*, **60**, 1124.
157. Jost, D., Lüthy, W., Weber, H.P., and Salathe, R.P., 1986, *Appl. Phys. Lett.*, **49**, 625.
158. Shmidt, M. and Dransfeld, K., 1982, *Appl. Phys. A*, **28**, 211.
159. Emel'yanov, V.I. and Uvarova, I.F., *Acoust. Journal*, **31**, 481 (in Russian).

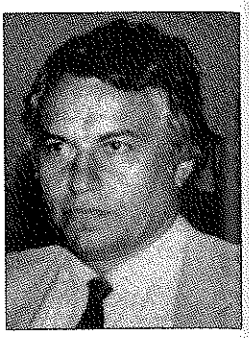

VLADIMIR I. EMEL'YANOV graduated from the Physics Faculty of Moscow State University and received a Candidate's (1973) and Doctor of Science degree (1988) in laser physics from the same university. He is now a professor at the International Laser Center, Moscow State University. His main fields of research include the cooperative and coherent phenomena in optics and the interaction of high-power laser radiation with solid surfaces.

He coauthored more than 150 original papers and three monographs on laser physics: *Cooperative Phenomena in Optics* (1988, Moscow: Nauka, in Russian); *Interaction of Strong Laser Radiation with Solids and Nonlinear Optical Diagnostics of Surfaces* (1990, Leipzig: Teubner, with S.A. Akhmanov and N.I. Koroteev), and *Superradiance and Light-Induced Phase Transitions* (1992, Bristol: Adam Hilger, in press).